Revista Mexicana de Astronomía y Astrofísica, 61, 11-24, (2025)

OPEN ACCESS https://doi.org/10.22201/ia.01851101p.2025.61.02.02

Asymmetry and Concentration Parameters for Dwarf Late-Type Spiral Galaxies

I. Vega-Acevedo[1], **A. M. Hidalgo-Gámez**[1] **and B. E. Miranda-Pérez**[1,2]

[1]*Departamento de Física, ESFM, Instituto Politécnico Nacional, México.*
[2]*Departamento de Matemáticas, ESIME, Instituto Politécnico Nacional, México.*

Keywords: *galaxies: dwarf, galaxies: irregular, galaxies: photometry, galaxies: star formation, galaxies: structure*

Abstract

We analyzed the asymmetry and concentration parameters in a sample of late-type spiral galaxies using V and R broadband images. Asymmetry values were computed for different rotation angles and radii, revealing low asymmetry overall, with smaller values in the inner regions. No preferred angle significantly affected the asymmetry measurements. The concentration indices lie between those of large spirals and irregular galaxies. We compared our sample distribution in the $C-A$ plane with other late-type systems (dwarfs and normal spirals). Additionally, we explored the correlations between asymmetry and star formation rate and between concentration and stellar mass, contrasting our results with those of prior studies.

Resumen

En este trabajo se estudian los parámetros de asimetría y concentración en una muestra de galaxias espirales tardías, utilizando imágenes en bandas V y R. La asimetría se calculó para distintos ángulos y radios, mostrando valores bajos (especialmente en regiones internas), sin dependencia sistemática con el ángulo. La concentración presenta valores intermedios entre galaxias espirales grandes e irregulares. Analizamos la distribución de estas galaxias en el plano $C-A$ en comparación con espirales normales y enanas. Además, exploramos las correlaciones entre asimetría y tasa de formación estelar y entre concentración y masa estelar, contrastando nuestros resultados con estudios previos.

Corresponding author: I. Vega-Acevedo *E-mail address:* ivegaa@ipn.mx
Received: July 21, 2024 **Accepted:** March 27, 2025

1. General

Galaxies exhibit a wide variety of forms, and their classification is a challenging task. The classical classification method was introduced by Hubble (1936) and later refined by de Vaucouleurs (1959) is based on morphology. While this method is powerful, it has notable limitations, particularly its subjectivity, as the classification relies on the observer's judgement (Conselice et al., 2000b). Traditionally, this classification was based on photographic plate images, which are more sensitive to blue light. Consequently, blue filters are commonly used, as they emphasize star formation events, which are particularly important in late-type galaxies.

A new classification scheme was proposed by Conselice et al. (2000a), which relies on three parameters: concentration, asymmetry, and clumpiness, collectively known as the CAS system. Although related to morphology, these parameters are defined quantitatively, enabling a more objective classification of galaxies. This classification system was defined by Abraham et al. (1996b). Symmetry has long been a fundamental aspect of galaxy morphology but has often been overlooked in more detailed studies. Early papers on galaxy morphology, such as those by Curtis (1918) and Hubble (1926), described galaxies in terms of their symmetry, typically 180^o symmetry. In general, galaxies are dynamically relaxed systems, leading to a high degree of symmetry (Binney & Tremaine, 2008). Indeed, galaxy models often assume a symmetric mass distribution (Carroll & Ostlie, 2006). Understanding deviations from symmetry in the light distribution of galaxies can reveal underlying dynamical processes. For instance, galaxies affected by interactions or mergers tend to exhibit significant asymmetries (Conselice et al., 2000b).

Schade et al. (1995) first introduced the quantitative use of asymmetry as a morphological parameter to characterize distant galaxies observed with the Hubble Space Telescope (HST). Subsequent studies by Abraham et al. (1996a), Abraham et al. (1996b) and van den Bergh et al. (1996) utilized asymmetry to broadly classify distant galaxies within the Hubble Sequence framework.

Concentration, on the other hand, was initially employed by Morgan (1958, 1959) to develop a more refined classification model. More recently, it has been used to explore the central regions of galaxies, uncovering correlations between concentration and properties, such as X-ray flux (Pović et al., 2009) and central black hole mass (Graham et al., 2001a).

As mentioned, Conselice et al. (2000a) used these three parameters (considering the clumpiness, which is not included in the present investigation) for an alternative classification of galaxies using a sample of galaxies of all morphological types. These parameters can be easily determined from direct images in broadband images. In addition, they seem to be related to the intrinsic properties of galaxies, such as the color index, $(B-V)$, or the absolute magnitude, M_B (Conselice, 2003). He concluded that such classification can be as useful as the Hubble classification, since galaxies with similar CAS values might have similar properties. In his investigation, only two of the galaxies in his sample were classified as Sm (NGC 4861 and NGC 5204), and another two were classified as Sdm. This is not unusual because Sm and dS galaxies are underrepresented in the samples used for asymmetry determination, and they are considered as late-type galaxies in general. They are expected to have concentration and asymmetry parameters midway between those of Sd and irregular galaxies because they have looser spiral arms than other spirals (Sa-Sd), but they are not as disordered as irregular galaxies, and their bulges are quite dim when present.

In this study, we focus on the asymmetry and concentration parameters of a sample of Sm and dS galaxies to determine their proper placement in the $C-A$ diagram. These galaxies have traditionally been located within the late-type galaxy locus (e.g. Conselice 2003), despite the fact that star formation is not confined to the spiral arms but rather extends throughout the entire disk, albeit in a non-homogeneous manner. In fact, H II regions are not uniformly distributed across the galaxy, as observed in other spirals (Magaña-Serrano et al., 2020). Such characteristics may significantly influence the asymmetry and concentration parameters, potentially altering their position in the $C-A$ plane.

We also examined the variations in both asymmetry and concentration parameters depending on the filter used, as well as the effects of rotation angle and radius. In previous studies, only a 180^o rotation have been considered, with the exception of Conselice et al. (2000b) and Abraham et al. (1996a). Notably, most investigations have reported that asymmetry values strongly depend on the rotation angle, with most galaxies appearing nearly symmetrical under a 180^o rotation but not at other angles. This effect may be particularly relevant when emissions from star-forming regions dominate the total flux in certain bands, such as the B band or bluer wavelengths, which is typically the case for Sm and dS galaxies.

Additionally, the flux in the red bands is primarily determined by the underlying stellar population, which is more smoothly distributed throughout the disk (Conselice et al., 2000b). While this phenomenon occurs in all star-forming galaxies, it may be more pronounced in Sm and dS galaxies because of their smaller size relative to other spiral types but comparatively high star formation rates. Consequently, the observed differences in the asymmetry and concentration parameters could be more significant in these galaxies.

Finally, we obtained the dependence of the A and C values on the star formation rate and stellar mass, respectively, and compared them to those obtained for larger galaxies by Conselice (2003) and for tidal dwarf galaxies by Vega-Acevedo & Hidalgo-Gámez (2022).

The manuscript is structured as follows: § 2 describes the sample of galaxies studied as well as the data used for the determination of the parameters. In § 3, a brief description of the determination of the A and C values is presented, while the results, general as well as with different filters, angles, and radii, are presented in § 4. Finally, a discussion on the location of these galaxies in the $C-A$ plane is presented in § 5 as well as the relationship between the A and C parameters with some other characteristics of the galaxies. Finally, our conclusions are presented in § 6.

2. Observations and Data Reduction

The observations of the galaxies analyzed in this study were obtained by one of the authors using the 1.5m telescope at the OAN-SPM during two separate observation campaigns: March 7-9 and November 1-4, 2002. During both campaigns, most nights were not entirely photometric due to the presence of high clouds. However, the extinction was sufficiently low to obtain accurate flux measurements.

Table 1 summarizes the observations of the sample of dwarf spiral galaxies studied in this investigation. Column (1) lists the galaxy name, Columns (2) and (3) provide the exposure time for the R and V filters, respectively, Column (4) presents the signal-to-noise (S/N) ratio, Column (5) contains the seeing conditions, and Column (6) shows the air mass.

Data reduction and calibration were performed using the ESO-MIDAS software following standard procedures (Banse et al., 1983; Warmels, 1992). Atmospheric corrections were applied using the tables for the San Pedro Mártir Observatory (Schuster & Parrao, 2001). Several standard stars were used for flux calibration.

Figures (1) and (2) display the calibrated V-band images of the galaxies UGC 9570 and UGCA 74, respectively in the V filter.

The intensities in these images were normalized relative to I_0, which corresponds to the pixel located at the defined central position. The process for determining this central point is detailed in § 3. To avoid interference with the center determination, which could affect the asymmetry parameter measurements, bright foreground stars were

Table 1. Sample of dwarf spiral galaxies.

Galaxy[1]	Integration time[2]		SNR[3]	seeing[4]	Air mass[5]
	R	V		$[arcsec]$	$[mag]$
UGCA 5	1200	···	9.5	1.6	1.730
UGCA 74	1000	1200	9.7	1.8	1.840
UGC 891	1000	1200	8.7	1.5	1.260
UGC 2301	1100	1200	8.8	1.6	1.090
UGC 3775	1200	1200	9.1	1.9	1.120
UGC 5242	1200	1000	10.0	1.9	1.570
UGC 5296	1400	1200	4.1	2.0	1.178
UGC 6205	1600	1200	6.1	1.6	1.049
UGC 6304	1200	1200	4.0	1.7	1.280
UGC 9570	1200	1200	4.5	1.6	1.135
UGC 11820	1200	900	8.0	1.9	1.270
UGC 12212	1000	1200	9.2	1.8	1.010

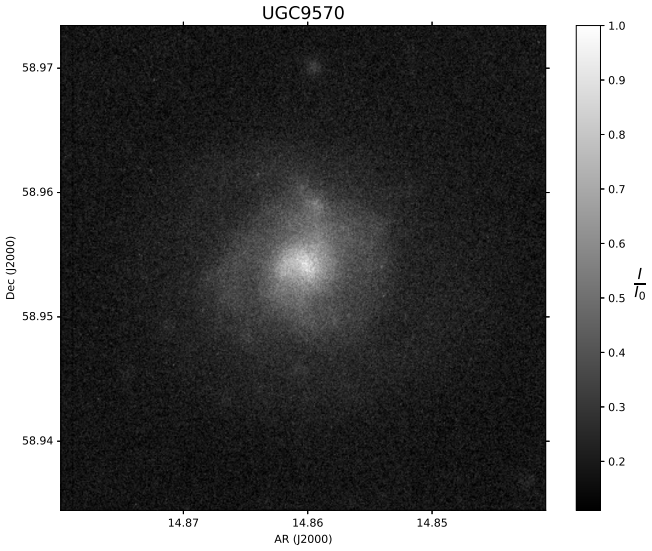

Figure 1. Reduced image of the galaxy UGC 9570 in the V filter observed at OAN-San Pedro Martir. The intensity in the image is normalized with respect to I_0 (see § 3).

removed and replaced by interpolating the background emission.

2.1. Sample description

All galaxies analyzed in this study were selected from the list of dwarf spiral galaxies compiled by Hidalgo-Gámez (2004), except for UGC 2301, which is a dS candidate. Thus, all of them are classified as dS, although UGCA 74 is categorized as a peculiar galaxy. Four of these galaxies (UGCA 5, UGCA 74, UGC 891, and UGC 5242) are considered barred galaxies (de Vaucouleurs et al., 1991).

Table 2 presents some of the main properties of the galaxies in our sample. Column (1) lists the galaxy name, while Columns (2) and (3) provide the right ascension (α) and declination (δ) coordinates, respectively. Column (4) lists the inclinations. Most of the galaxies are either

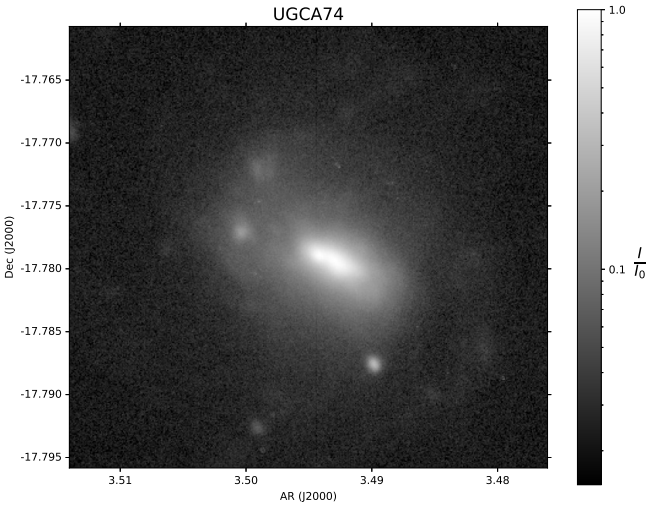

Figure 2. Reduced image of the galaxy UGCA 74 in the V filter observed at OAN-San Pedro Martir. The intensity in the image is normalized with respect to I_0 (see § 3).

face-on or have an intermediate inclination, with values ranging from 14^o to 56^o. Only two galaxies, UGC 891 and UGC 2301, exhibited high inclinations. This is a relevant factor, as lower inclinations facilitate the determination of both the asymmetry and concentration parameters. The two highly inclined galaxies were retained in our sample to assess the impact of inclination on the measurement of these parameters. Columns (5), (6), and (7) provide the optical radius, distance, and absolute magnitude (M_B), respectively. The radii and absolute magnitudes were determined following Hidalgo-Gámez (2004), incorporating the latest distance measurements from NED-NASA. Galactic extinction corrections were applied to these calculations. Finally, the last column presents the morphological classification according to NED-NASA.

With this homogeneous although small sample, it is very interesting to study the asymmetry and concentration parameters and check if dS are located near the spiral galaxies or closer to the locus on irregular ones in the $C-A$ plane.

3. Determination of the A and C parameters

3.1. Where is the center?

To determine both the asymmetry and concentration parameters, it is necessary to determine the center of the galaxy.

In this investigation, the weighted center (C_w), defined as the point obtained by weighting the pixel intensities in a specific region, was chosen instead of the photometric center because it can be determined more easily without additional processing. The distance between the weighted center and the photometric center in these galaxies is less than the seeing (Vega-Acevedo, 2013). The weighted center,

Table 2. Galaxy sample

Galaxy[(1)]	$\alpha^{(2)}_{J2000}$	$\beta^{(3)}_{J2000}$	$r^{(4)}_{25}$ [kpc]	D[(5)] [Mpc]	$M^{(6)}_B$	Morphology[(7)]
UGCA5	00h18m48.3s	-19d00m28s	9.14	42.5±	-18.46	SAB(s)m
UGCA74	03h29m31.7s	-17d46m42s	4.5	20.5±	-18.05	SB(s)c pec
UGC891	01h21m18.9s	+12d24m43s	1.62	4.86±	-14.28	SABm
UGC2301	02h49m38.2s	+38d15m41s	⋯	⋯	-18	dwarf*
UGC3775	07h15m52.6s	+12d06m54s	7.69	34.1	-16.56	Sm
UGC5242	09h47m05.5s	+00d57m51s	6.36	32.4	-17.75	SB(s)m
UGC5296	09h53m11.6s	+58d28m42s	3.65	24.5	-15.54	Sm
UGC6205	11h09m58.3s	+46d05m42s	6.37	24.0	-17.13	Sm
UGC6304	11h17m49.1s	+58d21m08s	5.67	28.3	-15.84	Sm
UGC9570	14h51m35.9s	+58d57m14s	⋯	33.5	-16.22	dS*
UGC11820	21h49m28.4s	+14d13m52s	3.22	11.3	-14.20	Sm
UGC12212	22h50m30.3s	+29d08m18s	1.82	8.1	-14.04	Sm

[a]Column (1) is the name of the galaxy, Columns (2) y (3) are the right ascension and declination respectively in $J2000$, Column (4) is the mayor axis, the distance of galaxy is in Column (5) and Column (6) is the absolute magnitude in B, using the most recent distance determination, and Column (7) is the morphological classification (de Vaucouleurs et al., 1991; Nilson, 1973).

$C_w = (C_{w,x}, C_{w,y})$, was obtained as:

$$C_w = (C_{w,x}, C_{w,y}) = \frac{\left(\sum_{i,j}(x_i I_{i,j}), \sum_{i,j}(y_j I_{i,j})\right)}{I}, \quad (1)$$

where the $I_{i,j}$ is the intensity of each pixel located in (i,j), and x_i, y_j are the coordinates of the pixel (i,j), the $\sum(x_i I_{i,j})$ is the sum of the product between the position in the x coordinate and the intensity in the position (i,j) and $I = \sum_{i,j} I_{i,j}$

The challenge in determining the weighted center, as previously mentioned, is the variation in the average intensity (and consequently, in the coordinates of the weighted center) caused by the presence of field stars near the galaxy. To mitigate this effect, these stars must be masked to eliminate their contributions.

In addition to determining the weighted center, it is also necessary to define the galaxy′s size for the calculation of the asymmetry (A) parameter. Following Conselice (2003), we adopted the Petrosian radius. To determine this radius, the surface brightness profile must be obtained (Graham et al., 2005), which in this study was modeled using Sérsic's law (Sérsic et al., 1968).

3.2. Asymmetry

The asymmetry parameter (A) quantifies the irregularity or unevenness of the brightness and structure of a galaxy across different regions. It measures the extent to which the shape of a galaxy changes during a specific rotation. Asymmetry can provide valuable insights into past dynamical events, such as galactic mergers or interactions with other galaxies, as interacting galaxies typically exhibit higher asymmetries. To determine this parameter, the luminosity distribution in the opposite regions of the galaxy was compared to identify imbalances in the light distribution. In this study, we proceeded as follows: First, the original image, Ima, was rotated by an angle, θ, counterclockwise, considering the weighted center as the rotation point. This rotated image is denoted as Rot. Then, the following operation was performed on the images:

$$A = \left|\frac{Rot - Ima}{Ima}\right| \quad (2)$$

Finally, the intensity of a region, centered at the weighted center and with a radii of the r_{25}, is measured at the image obtained from equation 2, which will be defined as parameter A (Abraham et al., 1996b). With that definition, the parameter takes values from 0 to 1, where 0 means a symmetric system under that rotation and 1 is a completely asymmetric one. In general, spiral galaxies are quite symmetric for a 180^o rotation, but they are asymmetric for 90^o or 45^o rotations. Elliptical galaxies are very symmetrical for most angles, with asymmetry values between 0.1 and 0.3. In contrast, irregular galaxies have average values of $0.4 - 0.5$ under all the angles (Conselice et al., 2000b; Abraham et al., 1996b).

In general, the asymmetry parameter is determined using a single angle, mostly 180^o, and a fixed size for every galaxy (Conselice, 2003), although some authors used several radii, filters, and angles to determine how this parameter changes. Hernández-Toledo et al. (2005) measured CAS parameters in BVRI bands for a sample of 66 galaxies and found that the differences in CAS parameters for paired galaxies from the B to I bands are, on average, small. In addition, only a single size of the galaxy was considered, although Conselice

et al. (2000b) concluded that the internal part of the galaxies might be more symmetrical.

3.3. Concentration

The concentration, C, of a galaxy refers to the relationship between the luminosity in its central core and the total luminosity along its extension. This parameter is useful for distinguishing between different types of galaxies, especially between elliptical and spiral galaxies. Higher values of C indicate that a larger amount of light in a galaxy is contained within its central region (for example, Bershady et al. 2000; Graham et al. 2001a, 2005). Elliptical galaxies tend to have a higher concentration because most of their light is centered in the nucleus, whereas spirals with extended arms have a lower value. The concentration is calculated as the ratio of two radii containing a specific percentage of the total luminosity of the galaxy. In this study, we use the definition by Conselice (2003) which quantifies how much light is at the center of a galaxy as opposed to its outer parts, that is

$$C = 5log\left(\frac{r_{80}}{r_{20}}\right), \quad (3)$$

In this equation, r_{80} and r_{20} are the radii enclosing the 80% and 20% of the total flux, respectively, respectively. To obtain these radii, we fit a Petrosian-type brightness profile to each galaxy under study and determined the integral of the profiles to obtain the radii that contain 20% and 80% of the total flux.

4. Results

4.1. Asymmetry for dwarf spiral galaxies

In this investigation, we used three different angles (45^o, 90^o, and 180^o), two filters (V and R) and two radii (r_p and $2r_p$) in the determination of the asymmetry. These configurations were employed to evaluate whether the conclusions drawn for large galaxies -such as lower asymmetry values in the inner regions, higher symmetry under a 180^o rotation, and minimal differences between filters- are consistent for smaller galaxies. The motivation for this comparison lies in the distinct structural differences: large galaxies typically exhibit a canonical spiral structure, whereas the smaller galaxies in our sample exhibit a looser spiral pattern with a more disordered light distribution.

The values of the asymmetry parameter for the sample in filters V and R at radii $r = r_p$ and $r = 2r_p$ are listed in Table 3. Column (1) has the galaxy name, Columns (2), (3), and (4) are the values for rotation angles 45^o, 90^o and 180^o in filter V, and Columns (5), (6), and (7) are the ones for rotation angles 45^o, 90^o and 180^o in filter R. The top part of this table shows the A values determined for a radius r_p, which considers the innermost part of the galaxy, while the values at the bottom correspond to $r = 2r_p$, which includes most of the total galaxy.

4.1.1. Asymmetry at different filters

As previously mentioned, the R filter is typically used for asymmetry determination because the luminosity from K-type stars, which dominate this filter, is assumed to be virialized, following a more symmetric and homogeneous distribution (Conselice, 2003). However, this assumption may not be entirely appropriate for star-forming galaxies. If the star formation rate (SFR) is sufficiently high, the R-filter emission may be contaminated by Hα line emission at 6562Å, originating from H II regions. Additionally, the scattered distribution and high luminosity of H II regions in Sm and dS galaxies could affect the weighted center determination, subsequently influencing the asymmetry. Since most of the galaxies in our sample are star-forming (Magaña-Serrano et al., 2020), a comparison with a bluer filter (V) allows us to assess the significance of these effects on the results.

As shown in Table 3, no significant differences in asymmetry values were observed between the two filters. A similar conclusion can be drawn from Figure 3, which plots the asymmetry values obtained with the R filter (y-axis) against those obtained with the V filter (x-axis) for all galaxies in the sample. The plot also includes the 1:1 reference line and the 1σ confidence interval (dotted lines) for the internal regions of the galaxies (r_p) across the three rotation angles used in this work. We focus on r_p because asymmetry values are generally lower in this region, making any differences more likely attributable to filter effects (See § 4.3). For completeness, a square-root function fit is shown as a dashed line.

At 90^o and 180^o there are four galaxies that do not fit into the 1σ. As one of the sources of asymmetry might be the distribution of the H II regions, those galaxies with the largest SFR might be those with the largest asymmetry. The galaxy with the largest differences in the A values between the filters in our sample, UGCA 74, is also the galaxy with the highest SFR ($0.186 M_\odot yr^{-1}$, Hodge & Kennicutt 1983).

These results are predictable because both filters have very close central wavelengths; therefore, the light in both is dominated by a similar stellar population, especially if the star formation rates are low. They are very similar to those obtained by Hernández-Toledo et al. (2005) and Conselice et al. (2000b), where the differences in the asymmetry between the values in the blue (B, g) and red (R, r) filters are smaller than 0.1.

4.1.2. Asymmetry at different radii

In contrast to intermediate (Sbc, Sc, Sd) types of galaxies, where the H II regions are preferably located along the spiral arms, the regions of star formation in late types are disorderly distributed throughout the galaxy (see, for example, Magaña-Serrano et al. (2020); Roye & Hunter (2000)). Moreover, Conselice et al. (2000b) concluded that the internal part of galaxies might be more symmetrical because the spiral pattern is clearer. Another reason is that, in general, in normal spiral galaxies, the number of H II regions is smaller in the internal part (Hodge &

Table 3. Summary of Asymmetry

Galaxy	*V* filter			*R* filter		
	45^o	90^o	180^o	45^o	90^o	180^o
	$r = r_p$					
UGCA 5	0.18 ± 0.01	0.23 ± 0.04	0.25 ± 0.04	...	...	...
UGCA 74	0.19 ± 0.02	0.28 ± 0.01	0.17 ± 0.02	0.21 ± 0.03	0.33 ± 0.02	0.49 ± 0.01
UGC 891	0.14 ± 0.02	0.18 ± 0.02	0.18 ± 0.02	0.13 ± 0.01	0.15 ± 0.01	0.17 ± 0.01
UGC 2301	0.2 ± 0.02	0.3 ± 0.01	0.13 ± 0.01	0.18 ± 0.01	0.29 ± 0.01	0.12 ± 0.01
UGC 3775	0.2 ± 0.01	0.28 ± 0.01	0.32 ± 0.01	0.23 ± 0.01	0.29 ± 0.01	0.32 ± 0.01
UGC 5242	0.09 ± 0.01	0.13 ± 0.01	0.16 ± 0.01	0.11 ± 0.04	0.14 ± 0.03	0.17 ± 0.03
UGC 5296	0.12 ± 0.01	0.11 ± 0.01	0.09 ± 0.02	0.16 ± 0.04	0.14 ± 0.05	0.09 ± 0.07
UGC 6205	0.07 ± 0.02	0.09 ± 0.01	0.07 ± 0.02	0.07 ± 0.01	0.08 ± 0.01	0.07 ± 0.01
UGC 6304	0.09 ± 0.01	0.11 ± 0.01	0.12 ± 0.01	0.09 ± 0.01	0.12 ± 0.01	0.12 ± 0.01
UGC 9570	0.07 ± 0.01	0.1 ± 0.01	0.09 ± 0.01	0.07 ± 0.04	0.08 ± 0.04	0.08 ± 0.04
UGC 11820	0.13 ± 0.02	0.15 ± 0.01	0.15 ± 0.01	0.10 ± 0.04	0.11 ± 0.03	0.10 ± 0.03
UGC 12212	0.12 ± 0.02	0.18 ± 0.01	0.22 ± 0.01	0.09 ± 0.04	0.14 ± 0.03	0.17 ± 0.02
	$r=2r_p$					
UGCA 5	0.25 ± 0.01	0.32 ± 0.01	0.37 ± 0.01	...	...	...
UGCA 74	0.36 ± 0.02	0.5 ± 0.02	0.34 ± 0.02	0.35 ± 0.01	0.51 ± 0.04	0.39 ± 0.04
UGC 891	0.18 ± 0.05	0.22 ± 0.04	0.18 ± 0.05	0.14 ± 0.04	0.17 ± 0.03	0.15 ± 0.03
UGC 2301	0.15 ± 0.02	0.32 ± 0.02	0.13 ± 0.02	0.13 ± 0.01	0.29 ± 0.01	0.12 ± 0.01
UGC 3775	0.28 ± 0.01	0.4 ± 0.01	0.49 ± 0.01	0.29 ± 0.01	0.41 ± 0.01	0.48 ± 0.01
UGC 5242	0.13 ± 0.04	0.17 ± 0.03	0.16 ± 0.03	0.15 ± 0.02	0.21 ± 0.01	0.19 ± 0.01
UGC 5296	0.11 ± 0.04	0.14 ± 0.03	0.13 ± 0.04	0.12 ± 0.02	0.15 ± 0.01	0.14 ± 0.01
UGC 6205	0.11 ± 0.03	0.14 ± 0.02	0.08 ± 0.04	0.1 ± 0.01	0.13 ± 0.01	0.08 ± 0.02
UGC 6304	0.11 ± 0.02	0.13 ± 0.02	0.12 ± 0.02	0.11 ± 0.03	0.15 ± 0.02	0.14 ± 0.02
UGC 9570	0.08 ± 0.03	0.11 ± 0.03	0.11 ± 0.02	0.08 ± 0.01	0.1 ± 0.01	0.1 ± 0.01
UGC 11820	0.15 ± 0.01	0.18 ± 0.01	0.21 ± 0.01	0.19 ± 0.02	0.20 ± 0.01	0.22 ± 0.01
UGC 12212	0.17 ± 0.02	0.24 ± 0.01	0.3 ± 0.01	0.16 ± 0.01	0.23 ± 0.01	0.29 ± 0.01

Top: Asymmetry for a $r = r_p$.
Bottom: Asymmetry for a $r = 2r_p$.

Kennicutt, 1983). Then, a difference in the asymmetry values is expected between the internal and external parts for late-type galaxies.

This is clearly seen in Figure 4, where the *A* values in the external parts ($2r_p$) are shown against the internal parts (r_p) in *R* filter. Along with the data points, the identity and 1σ lines are shown for the three angles studied here, as well as the square root fitting (dashed line).

Approximately half of the galaxies in the sample have differences in the *A* values larger than 1σ. Interestingly, galaxies with low asymmetry values, such as UGC 11820 and UGC 5242, show large differences between their inner and outer parts. Three of the four barred galaxies in our list have large differences in radius. The other galaxy, UGC 891, has a large inclination, which might cover the differences. The two galaxies with the largest inclination have the smallest differences in *A* between r_p and $2r_p$ when the average values in the filter and angle are considered for every radius.

Another reason for the increase in the *A* parameter with radius might be the interactions, present or past, suffered by the galaxies. The only peculiar galaxy in our sample that might be interacting is UGCA 74, which shows large differences and also has the largest SFR, as previously mentioned. Therefore, it can be concluded that barred galaxies or those in interaction or with an intense event of star formation are expected to show large differences in asymmetry between their inner and outer parts.

4.1.3. Asymmetry at different angles

Classical spiral, two-arm galaxies have low values of asymmetry for a 180^o rotation (Conselice et al., 2000b). In contrast, late-type spiral galaxies have, in many cases, no clear spiral pattern, sometimes with an odd number of arms. Therefore, differences in the *A* parameter might be related to the spiral structure of the galaxies. Both, Abraham et al. (1996a) and Conselice et al. (2000b) found that the asymmetry strongly depends on the angle of rotation if

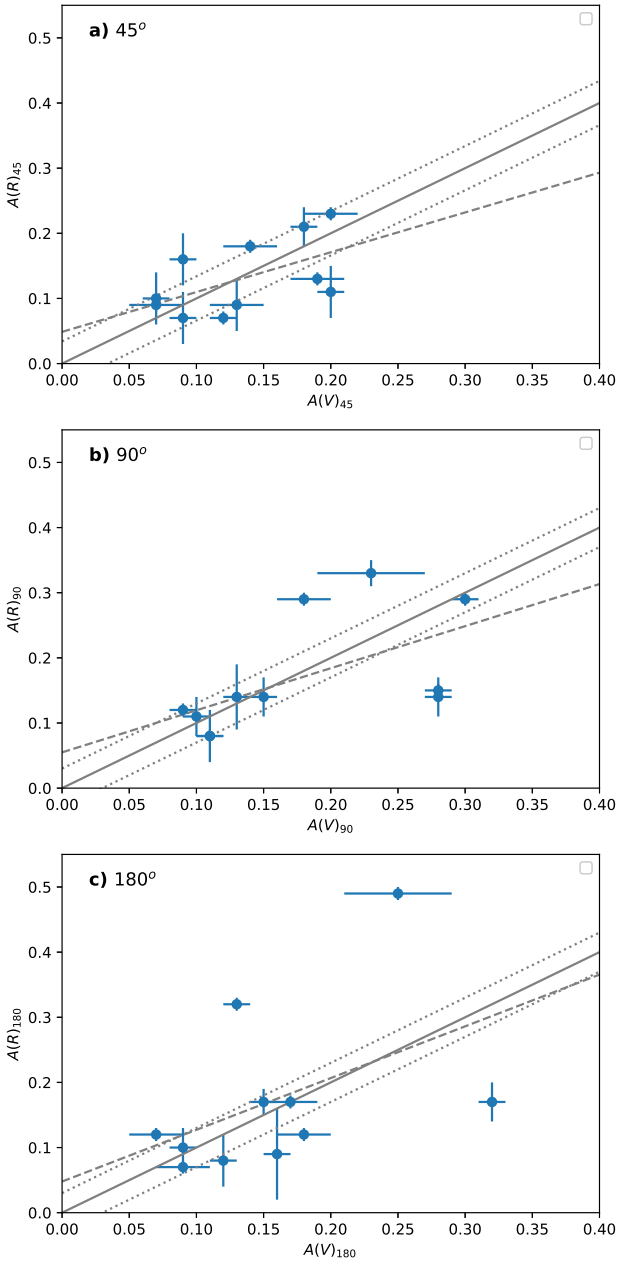

Figure 3. Comparison of asymmetry values for the galaxies in the sample in filter R versus filter V at r = r_p. The top panel (a) is for a rotation angle of 45^o, the middle panel, (b), for a 90^o angle and the bottom one, (c), for a 180^o angle.

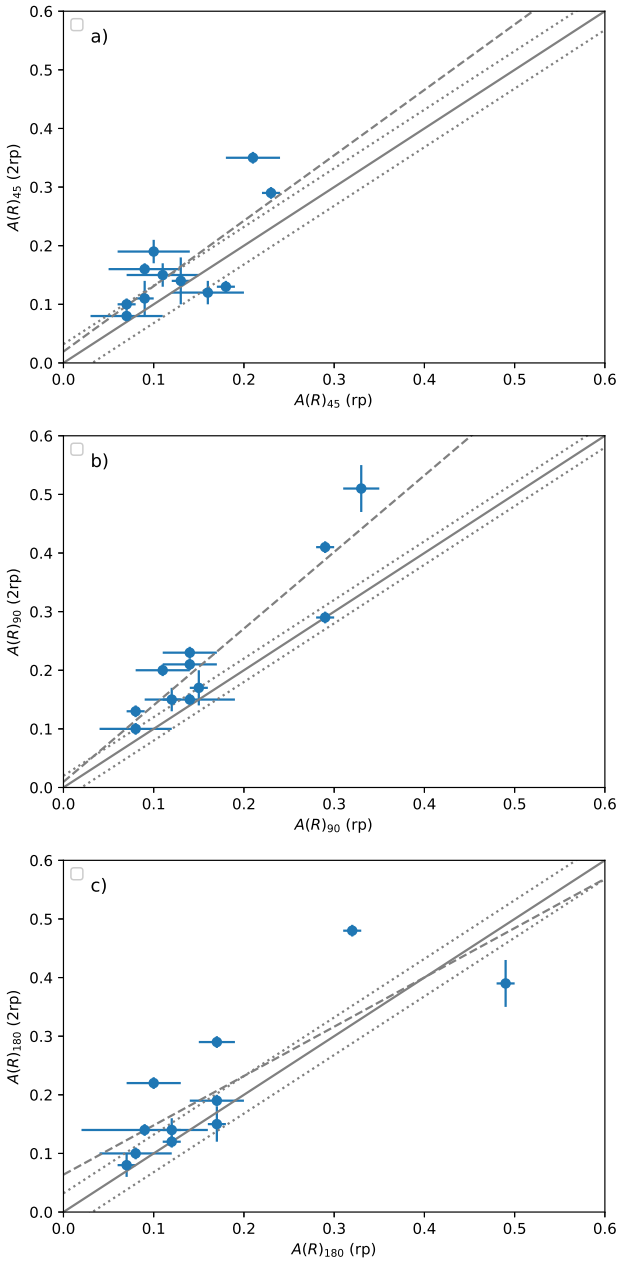

Figure 4. Comparison of the asymmetry values between the 2r_p versus 1r_p in filter R. The top panel, (a), is for a rotation angle of 45^o, the middel one, (b), shows values for a rotation angle of 90^o and the bottom one, (c), is for a rotation angle of 180^o.

the galaxy is very asymmetric. Finally, they concluded that the 180^o rotation was always the angle that gave the lowest asymmetry value, and such angles might indicates the existence of an axis of symmetry (Hernández-Toledo et al., 2005).

The asymmetry values for these three angles are listed in Table 3 for the different filters and radii, and they are plotted in Figure 5, with the identity and 1σ and squared fitting lines. Only the internal values of the asymmetry and the V filter were considered. Again, approximately half of the galaxies in the sample are not enclosed by the 1σ lines, but only four of them have differences larger than 2σ: UGCA 74, UGC 2301, UGC 3775, and UGC 12212. Smaller differences are present for asymmetries lower than 0.2 independently of the rotation angles considered (see Figure 5). Conselice et al. (2000b) have much larger differences in the asymmetry parameter for the majority of the galaxies in their sample.

Conselice et al. (2000b) also concluded that a 180^o rotation is particularly sensitive to interactions, whereas

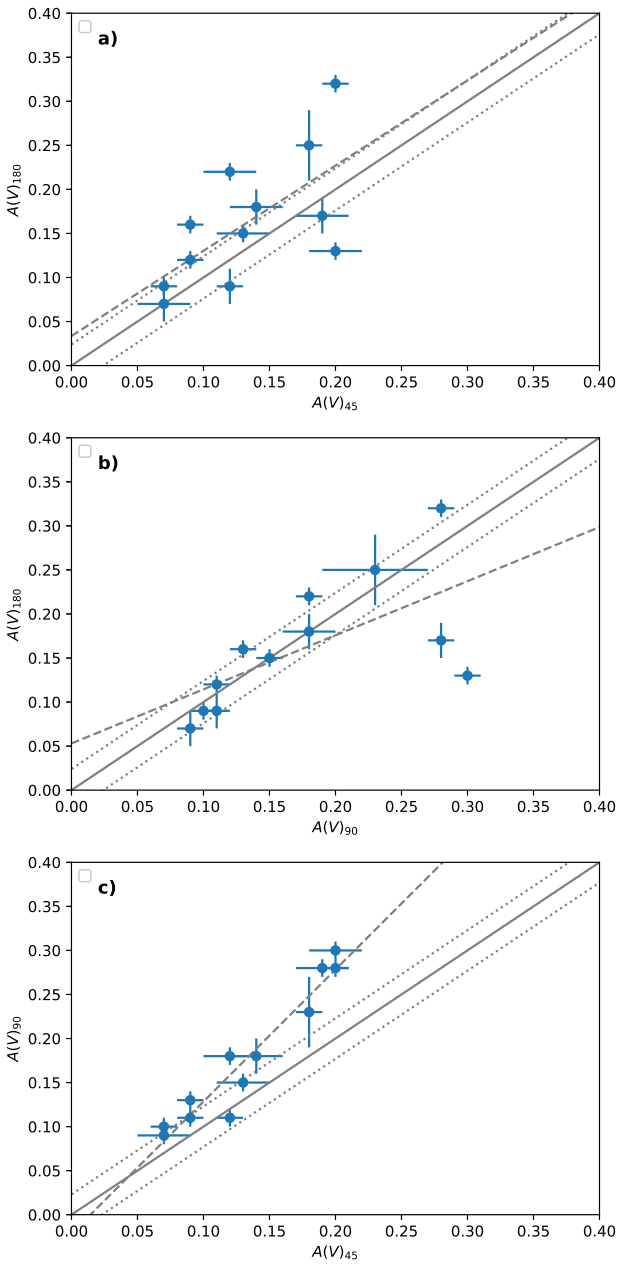

Figure 5. Comparison of asymmetry values in filter V at $r = r_p$ for different rotation angles. (a) rotation angles of 180^o vs 45^o, (b) rotation angles of 180^o vs 90^o and (c) rotation angles of 90^o vs 45^o.

higher asymmetry (A) values at 90^o or 45^o are primarily associated with star formation. Furthermore, asymmetry at 180^o correlates with morphological type, interactions, and color index ($B-V$), while the maximum asymmetry at 90^o is related to the axis ratio b/a; specifically, larger asymmetry values correspond to larger axis ratios.

Finally, the minima of the asymmetry parameter across the full rotation range (1^o to 360^o) may be linked to the number of spiral arms. In particular, a minimum at 90^o suggests the presence of a four-arm structure.

According to Table 3 (upper half, Columns 5, 6 and 7), only three galaxies have a maximum of the asymmetry at 180^o (UGCA 74, UGC 3775 and UGC 12212) however, only one of these galaxies might be in interaction and their only morphological difference is that UGCA 74 is a barred galaxy. Its color, of 0.49, is much larger than the value expected from its asymmetry, according to Figure 10 in Conselice et al. (2000b). Two of these galaxies have a similar b/a axis ratio of $0.12-0.13$ while there is no information on the third. UGCA 74 has a much larger asymmetry than expected from its low axis ratio, according to Figure 13 in Conselice et al. (2000b).

Only one galaxy has the maximum at 90^o (UGC 2301) with a axis ratio of 0.4. Finally, none of the galaxies in our sample had a maximum at 45^o. Moreover, the remaining galaxies in the sample have very similar values for all the angles studied. It is interesting to note that five of the galaxies show an increment of the asymmetry for larger rotation angles, while only one shows the contrary trend.

4.2. Concentration for dwarf spiral galaxies

The concentration parameter, as already mentioned, is related to some of the intrinsic properties of galaxies, such as dispersion velocity, size, and luminosity (Graham et al., 2001b). Moreover, it is well known that the earlier the galaxy, the larger the C values (for example Conselice, 2003, and references therein). The average value for elliptical galaxies is approximately 4.4 while for dE is 2.5 and for dI is 2.9. Hernández-Toledo et al. (2005) showed that the average concentration parameter decreases from the I to the B bands, in agreement with the finding that galaxy light distributions are more extended (less concentrated) in bluer bands than in red bands (de Jong, 1996).

Table 4 presents the concentration C values for the galaxies in our sample, determined as described in § 3, for the V filter (Column 2) and the R filter (Column 3). The first notable observation is that the C parameter remains nearly identical for both filters. This similarity may be attributed to the close central wavelengths of these filters, which result in minimal differences in galactic morphology. Furthermore, the average C value for our sample is 2.7 (see Table 5) in both filters, placing these galaxies at an intermediate level between dI and dE types but significantly lower than the average value for classical spirals (3.9 according to Conselice 2003).

Only two galaxies, UGCA 74 and UGC 2301, exhibit higher C values, while UGC 12212 has a value lower by more than 1σ. The high concentration values observed in UGCA 74 and UGC 2301 bring them closer to those of elliptical galaxies, whereas UGC 12212 displays a concentration even lower than that of Tidal Dwarf Galaxies (see Vega-Acevedo & Hidalgo-Gámez 2022). Among these three galaxies, only UGCA 74 shows high asymmetry values in its outer regions, suggesting that its elevated C values may be linked to a central star formation event triggered

Table 4. Concentration, C

Galaxy	C_V	C_R
UGCA 5	2.5±0.2	···
UGCA 74	4.1±0.3	3.9±0.2
UGC 891	3.3±0.2	3.3±0.3
UGC 2301	4.4±0.1	4.3±0.2
UGC 3775	2.4±0.2	2.2±0.2
UGC 5242	1.9±0.3	1.9±0.1
UGC 5296	2.0±0.2	1.9±0.3
UGC 6205	2.1±0.1	2.1±0.2
UGC 6304	1.9±0.2	1.9±0.3
UGC 9570	2.0±0.1	2.0±0.1
UGC 11820	3.0±0.3	3.0±0.2
UGC 12212	1.3±0.2	1.3±0.2

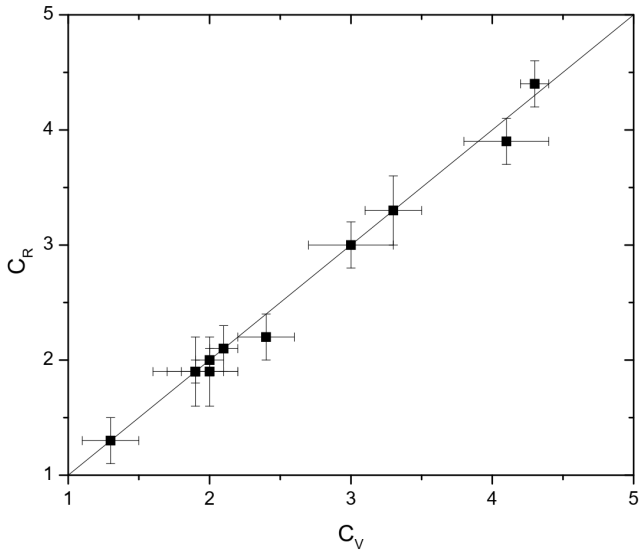

Figure 6. Plot of concentration in filter V versus concentration in filter R. The line represent a correlation one-by-one.

by an ongoing interaction. Notably, the other two galaxies also exhibit peculiar asymmetry values.

Figure 6 illustrates that the concentration values in the V and R filters follow a linear one-to-one correlation.

5. Discussion

As discussed previously, the main goal of this investigation is to determine the A and C parameters for a sample of dS galaxies and compare them with the values for other types of galaxies. In the previous sections, we obtained the asymmetry and concentration parameters, and the average values are of 0.18±0.02 and 2.55±0.02, respectively, considering the R filter, r_p and a 180^o angle.

We can compare these average values of C and A with those reported by Conselice (2003) (See Table 5). The concentration values for dS galaxies are very similar to those of dE and starburst galaxies and are slightly lower

Table 5. Averages and 1σ variations of C and A for Galaxy Types

Type	C	A
Ellipticals[a]	4.47±0.27	0.02±0.02
Early-type disks (Sa-Sb)[a]	3.75±0.59	0.07±0.04
Late-type disks (Sc-Sd)[a]	3.10±0.47	0.15±0.06
Irregulars[a]	3.25±0.69	0.33±0.26
Edge-on disks[a]	3.7±0.6	0.17±0.11
ULIRGs[a]	3.56±0.74	0.32±0.19
Starbursts[a]	2.7±0.2	0.53±0.22
Dwarf ellipticals[a]	2.46±0.28	0.02±0.02
Dwarf irregular[a]	2.87±0.30	0.18±0.10
TDG[b]	1.75±0.27	0.46±0.22
Dwarf spiral [c]	2.36±0.60	0.22±0.13

[a] From Conselice (2003).
[b] From Vega-Acevedo & Hidalgo-Gámez (2022).
[c] This work.

than those of dI galaxies. In contrast, these values differ significantly from those of late-type spirals. This suggests that, in terms of light concentration, dS galaxies resemble other dwarf galaxies more closely than larger spirals. Regarding asymmetry, the differences between dS and late-type spirals are smaller, yet the asymmetry values for dS and dI galaxies remain similar. Although it is difficult to distinguish between dS and late-type disk galaxies based solely on these data, it is notable that the C and A values of dS galaxies align more closely with those of dI galaxies than with those of late-type disks, as reported by Conselice (2003).

The reader may be concerned about the dispersion in the values presented here, particularly in the average values listed in Table 5. Although the 1σ dispersion for dwarf spiral galaxies is relatively large, it is not greater than the dispersion reported by other authors for half of the galaxy types studied (Conselice, 2003). Additionally, while the sample analyzed in this study is small (consisting of only 12 galaxies), it is comparable in size to the sample of dwarf elliptical galaxies and twice as large as the sample of starburst galaxies in Conselice′s work.

5.1. The A-C plane for late-type galaxies

The $A-C$ plane is a projection in two dimensions of the $C-A-S$ space described by Conselice (2003). It has been used to differentiate galaxies with different morphological types in a three-dimensional space (Conselice, 2003; Hernández-Toledo et al., 2005). It has been proven to be quite successful when high-redshift galaxies are studied because of the difficulties in their morphological classification. Therefore, it can be useful to shed light on the true nature of dS galaxies, as discussed in Hidalgo-Gámez (2004).

Figure 7 presents the $C-A$ plane for the galaxies in our sample. In addition to the data points for dS galaxies

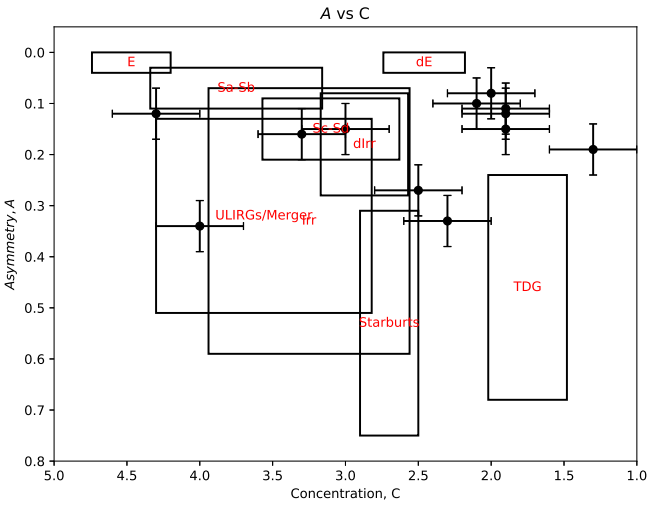

Figure 7. Plane $C-A$. The regions are centered on the average values of asymmetry, A, and concentration, C, for each galaxy type. The height and width of the regions correspond to the standard deviations of asymmetry and concentration, respectively. The values used for elliptical, E, dwarf elliptical, dE, spirals, S, early and late, dwarf irregulars, dIrr, starbursts, mergers, and URLIGS were taken from Conselice (2003). The data for TDGs from Vega-Acevedo & Hidalgo-Gámez (2022). Data for dwarf spiral, dS, were taken from Table 3 for r_p at filter V and Table 4 at filter V.

from Table 6, the regions occupied by different galaxy types, as defined by Conselice (2003) are also shown. Two main conclusions can be drawn: 1) There appear to be two distinct subsamples of dS galaxies: one clustering around $C = 2$ and another more widely distributed across the plane. 2) When considering the regions occupied by different morphological types, a continuous sequence is evident, extending from elliptical galaxies (located in the upper left of 7) toward dS and dE galaxies (upper right). Additionally, mergers, starburst galaxies, ULIRGs, TDGs, and some dS galaxies seem to form a parallel sequence at higher asymmetry values.

Overall, dS galaxies are widely scattered in the $C-A$ plane. Some exhibit values similar to those of dwarf elliptical galaxies, whereas the rest are broadly distributed. Specifically, two galaxies (UGCA 5 and UGC 3775) have high asymmetry (A) but normal concentration (C), whereas UGC 2301 and UGCA 74 display high C values, resembling elliptical galaxies, although UGCA 74 falls within the ULIRG region. In addition, two galaxies (UGC 891 and UGC 11820) lie at the boundaries of the starburst galaxy region.

However, the large dispersion in the $C-A$ plane is not exclusive of dS galaxies. All the groups are quite scattered in the $C-A$ plane, except for giant and dwarf elliptical galaxies, which occupy a small part of the plane.

5.2. Extreme galaxies

We have noticed along this investigation the anomalous A and C values of some of the galaxies, which can be seen in Figure 7. Two galaxies lie at the intersection of the late-type spiral and irregular galaxies (UGC 891 and UGC 11820). Another two have the most extreme concentration values but with the same asymmetry (UGC 2301 and UGC 12212). One more, UGCA 74, is inside the ULIRGs region, and UGCA 5 and UGC 3775 are at the edge of the starburst galaxies region. Finally, five of the galaxies (UGC 5242, UGC 5296, UGC 6205, UGC 6304, and UGC 9570) are located close to the dE.

In order to understand the location of the galaxies in the sample on the $C-A$ plane, we can study them in detail. From the values listed in Tables 3 and 4, we see that there are few galaxies with anomalous values of C and A: two of them (UGC 2301 and UGCA 74) have C values very similar to elliptical galaxies, while another two (UGCA 5 and UGC 3775) have A values similar to the starburst galaxies.

The large concentration value of UGC 2301 resides in its round, low surface brightness shape, while the small asymmetry value is due to its lack of any structure. In contrast, UGCA 74 is a barred galaxy classified as peculiar, with a clear single arm; therefore, its large A value places it in the ULIRGs locus. Moreover, it has the largest SFR of the galaxies in the sample ($0.186 M_\odot yr^{-1}$ Parkash et al. (2018)). Concerning the galaxies in the starburst locus, UGCA 5 is an isolated galaxy (Karachentsev et al., 2006, 2003) with an arm or half-ring in the eastern part of the galaxy. There are several clumps with high emission in both the UV and B bands, but not in the R or NIR bands. These clumps, as well as the half-ring, are responsible for the large asymmetry. In contrast, UGC 3775 has an SFR typical of late-type galaxies ($0.06 M_\odot$ yr^{-1}; Magaña-Serrano et al. 2020) but with a round appearance. Therefore, despite the relationship between A and SFR, according to Conselice (2003), the location in the $C-A$ plane of UGCA 74, UGCA 5, or UGC 3775 is not because their SFR, which is actually much lower than in any starburst.

Another interesting group of galaxies comprises those with both low values of C and A which are located in the vicinity of the dE locus (UGC 5242, UGC 5296, UGC 6205, UGC 6304, and UGC 9570). In all cases, the low asymmetry and concentration values are due to their low surface brightness and lack of clear structures. Their SFR are similar to those of the galaxies in our sample belonging to the ULIRG and Starburst loci (see Magaña-Serrano et al. 2020).

5.3. Parameters affecting the C-A plane

Several parameters may influence the location of galaxies in the $C-A$ plane. One such factor is the presence of a bar. In our sample, only four galaxies are barred, and their average asymmetry parameter (A) is higher than that of non-barred galaxies (0.23 compared to 0.16). Two of these galaxies exhibited high asymmetry values, whereas the remaining

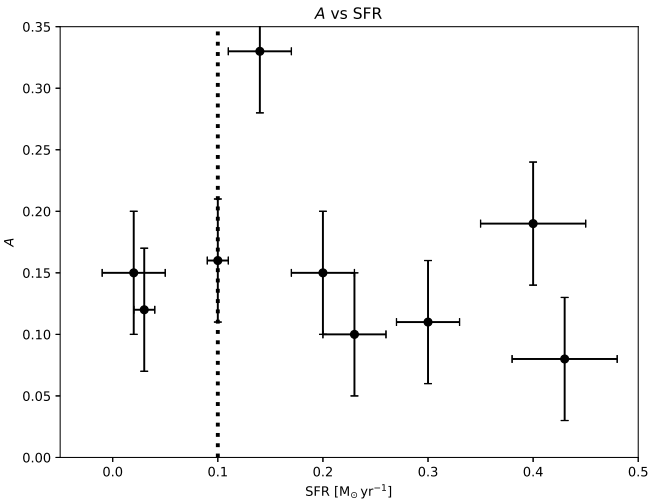

Figure 8. The relationship between the asymmetry at 180^o and the SFR for nine of the galaxies of the sample.

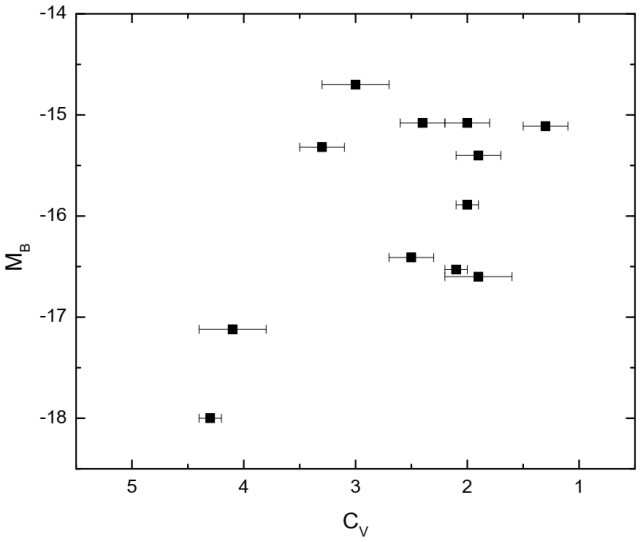

Figure 9. Plot of absolute magnitude B versus concentration in filter V.

two had intermediate values. Additionally, all galaxies with the lowest A values were non-barred.

Another factor that may affect the A value is the spiral structure of the galaxies. In a previous study of late-type galaxies by Magaña-Serrano et al. (2020), the spiral structure of eight of the 12 galaxies in our sample was analyzed. No strong correlation was found between the A parameter and the spiral structure. However, three of the four galaxies with no clear spiral structure have A values greater than 0.15.

According to Conselice et al. (2000a), A_{180} is sensitive to star-forming regions in galaxies. Therefore, a relationship between asymmetry and the star formation rate (SFR) might be expected. This relationship is shown in Figure 8 for nine galaxies in our sample. There is no clear relationship between these two parameters for these galaxies; instead, they show constant values. The galaxy with the largest SFR, UGC 9570, has a normal value of the A parameter.

In the classical work by Graham et al. (2001b), it was concluded that the concentration index is also a measure of the scale of a galaxy. Moreover, they argued that there is a correlation between the total light concentration and the stellar mass because elliptical massive galaxies have larger C values than spiral and irregular galaxies. In order to prove such a correlation for late-type galaxies, the stellar masses of some of the galaxies in the sample were estimated following the relationship between the M/L ratio (in solar units) and the AB magnitudes (from the SDSS RD7 corrected by Galactic extinction and K-correction) by Bell et al. (2003).

$$\log(M/L) = a_\lambda + (b_\lambda \times color) \quad (4)$$

A total of six different M_* values were determined from the $r-i$ and $r-z$ colors. The average of all these values was considered as the stellar mass of the galaxies. The uncertainties in the stellar masses were determined from the standard deviations of the results. The M_* values obtained are listed in Table 6.

The relationship between stellar mass and concentration in the R filter is shown in Figure 10. Although the sample size was small, a strong linear correlation was observed, with a regression coefficient of 0.86. However, the data exhibited significant dispersion. This result differs notably from the trend reported by Vega-Acevedo & Hidalgo-Gámez (2022), where the correlation was found to be exponential for galaxies with stellar masses below $2.4 \times 10^8 M_\odot$ and flat for higher masses (represented by the dashed line in the figure).

This finding is particularly intriguing given the subtle differences observed in the $C-A$ plane between the tidal dwarf galaxies and candidate galaxies analyzed by Vega-Acevedo & Hidalgo-Gámez (2022) and the dS galaxies in their study (see Figure 10). However, additional data on Sm and dS galaxies are required to establish a more conclusive relationship between these two parameters.

Finally, we briefly discuss the relationship between the SFR and stellar mass for the five galaxies with stellar mass values. This is shown in Figure 11. Although there are few data, a strong correlation between these two parameters for dS galaxies is clear. Again, more data on the stellar mass for dS galaxies are needed to check the trend emerging here.

6. Conclusions

In this study, the asymmetry and concentration parameters for a sample of Sm/dS galaxies were determined. The average asymmetry value for our sample falls between those of irregular galaxies and late-type spirals, indicating that these galaxies are less symmetrical than the latter class. Regarding concentration, the average value was lower (indicating a higher concentration) than that of both late-type spirals and irregular galaxies.

Table 6. Stellar mass and Star formation rate

Galaxy	$M_*\left[M_\odot\right]\times10^8$	$SFR\left[\mathrm{M_\odot yr^{-1}}\right]$	C_R	A
UGCA 5	⋯	⋯	2.5±0.2	0.26±0.04
UGCA 74	⋯	⋯	4.0±0.2	0.34±0.05
UGC 891	⋯	0.10±0.01	3.3±0.2	0.16±0.03
UGC 2301	⋯	⋯	4.3±0.1	0.20±0.05
UGC 3775	⋯	0.14±0.03	2.3±0.2	0.33±0.1
UGC 5242	3.67±1.09	0.20±0.03	1.9±0.2	0.15±0.02
UGC 5296	2.34±1.18	0.03±0.01	1.9±0.3	0.12±0.01
UGC 6205	5.77±2.92	0.23±0.03	2.1±0.2	0.09±0.01
UGC 6304	5.24±1.62	0.30±0.03	1.9±0.3	0.12±0.01
UGC 9570	1.20±4.66	0.43±0.05	2.0±0.1	0.09±0.01
UGC 11820	⋯	0.02±0.03	3.0±0.2	0.15±0.02
UGC 12212	⋯	0.40±0.05	1.3±0.2	0.19±0.04

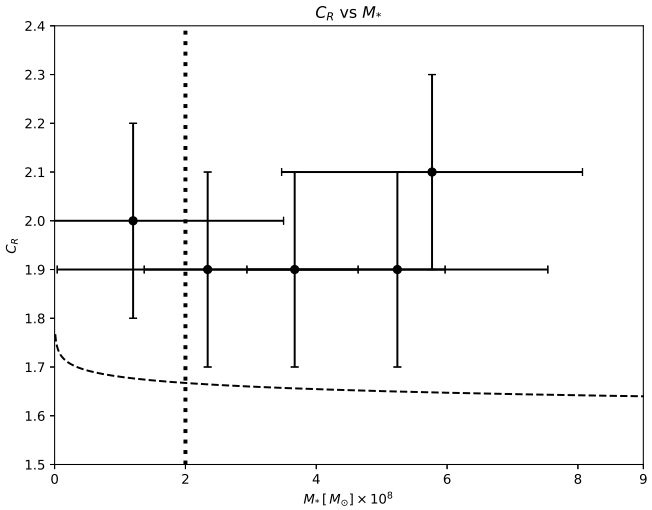

Figure 10. Concentration in R filter versus stellar mass. The dashed line is the correlation fit for TDG of Vega-Acevedo & Hidalgo-Gámez (2022).

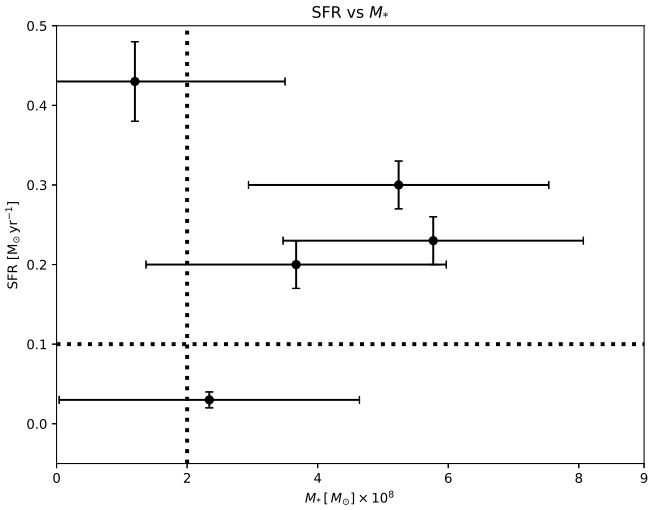

Figure 11. Plot of star formation rate versus stellar mass. The horizontal and vertical dash lines are the SFR and stellar mass mean of dwarf galaxies, respectively.

Additionally, we analyzed the variations in these parameters when different filters (V and R), rotation angles, and galaxy regions were considered. The data suggest that for Sm/dS galaxies, the asymmetry values do not exhibit significant differences between the two filters. However, variations were observed when different radii and angles were considered. The rotation angle yielding the lowest asymmetry was 45^o, while the highest asymmetry was found at 90^o at both radii. This behavior contrasts with that of large galaxies, possibly because of the looser spiral structure of smaller galaxies. Furthermore, the inner regions of galaxies are more symmetrical than the galaxy as a whole. This result aligns with the findings of Conselice (2003) on symmetry in the internal regions of galaxies.

The position of our sample in the $C-$A plane exhibits considerable dispersion, with some galaxies occupying the same locus as dE galaxies and others aligning with the starburst locus. However, the majority of the sample is located between the regions typically occupied by late-type spirals and irregular galaxies, as expected.

Finally, some interesting trends were noted regarding this sample of galaxies. There is a correlation between the concentration and stellar mass, but only for a few data points. Moreover, these galaxies are not in the same locus as irregular and TDG in this plane; instead, they align almost perpendicular to it. Considering asymmetry, there was no correlation between A and the SFR for the galaxies in our sample. The Sm/dS galaxies have, on average, similar values to those of the TDG, but the former do not show a bimodal behavior in the diagram. Finally, Sm/dS galaxies show a relationship between the SFR and stellar mass, being in between the two arms described by the TDG (Vega-Acevedo & Hidalgo-Gámez, 2022).

The discrepancies between the trends observed in our sample of Sm/dS galaxies and the results of previous studies are noteworthy and may suggest that these galaxies possess distinct structural properties, similar to those of TDG galaxies. This underscores the importance of detailed studies to better understand the specific characteristics of different galaxy types and how they vary in relation to properties, such as stellar mass and concentration.

Due to the small sample size (12 galaxies), the results are not statistically significant in this study. However, these findings are intriguing and warrant further investigation, particularly by expanding the sample size in future studies. Therefore, a larger dataset including dS, Sm, TDG, and dwarf irregular galaxies is essential for drawing more robust conclusions.

This research was supported by the Instituto Politécnico Nacional (México) under research projects SIP-20230588 and SIP-20240903. This work is part of M. en C. I. Vega Acevedo's Ph.D. thesis, sponsored by CONACyT (now SECIHTI). This investigation has made use of the NASA/IPAC Extragalactic Database (NED), which is operated by the Jet Propulsion Laboratory, California Institute of Technology, under contract with the National Aeronautics and Space Administration (NASA). This work is based in part on observations made with the GALEX Space Telescope, which is operated by the Jet Propulsion Laboratory of the National Aeronautics and Space Administration (NASA). The SDSS-III web site is http://www.sdss3.org/. SDSS-III is managed by the Astrophysical Research Consortium for the Participating Institutions of the SDSS-III Collaboration including the University of Arizona, the Brazilian Participation Group, Brookhaven National Laboratory, Carnegie Mellon University, University of Florida, the French Participation Group, the German Participation Group, Harvard University, the Instituto de Astrofísica de Canarias, the Michigan State/Notre Dame/JINA Participation Group, Johns Hopkins University, Lawrence Berkeley National Laboratory, Max Planck Institute for Astrophysics, Max Planck Institute for Extraterrestrial Physics, New Mexico State University, New York University, Ohio State University, Pennsylvania State University, University of Portsmouth, Princeton University, the Spanish Participation Group, University of Tokyo, University of Utah, Vanderbilt University, University of Virginia, University of Washington, and Yale University.

References

Abraham, R. G., Tanvir, N. R., Santiago, B. X., et al. 1996a, MNRAS, 279, L47, doi: 10.1093/mnras/279.3.L47

Abraham, R. G., van den Bergh, S., Glazebrook, K., et al. 1996b, ApJS, 107, 1, doi: 10.1086/192352

Banse, K., Crane, P., Grosbol, P., et al. 1983, Msngr, 31, 26

Bell, E. F., McIntosh, D. H., Katz, N., & Weinberg, M. D. 2003, ApJS, 149, 289, doi: 10.1086/378847

Bershady, M. A., Jangren, A., & Conselice, C. J. 2000, AJ, 119, 2645, doi: 10.1086/301386

Binney, J., & Tremaine, S. 2008, Galactic Dynamics: Second Edition (Princeton, NJ: PUP)

Carroll, B. W., & Ostlie, D. A. 2006, An Introduction to Modern Astrophysics (San Francisco: Addison-Wesley)

Conselice, C. J. 2003, ApJS, 147, 1, doi: 10.1086/375001

Conselice, C. J., Bershady, M. A., & Gallagher, III, J. S. 2000a, A&A, 354, L21, doi: 10.48550/arXiv.astro-ph/0001195

Conselice, C. J., Bershady, M. A., & Jangren, A. 2000b, ApJ, 529, 886, doi: 10.1086/308300

Curtis, H. D. 1918, PASP, 30, 159, doi: 10.1086/122707

de Jong, R. S. 1996, A&A, 313, 45, doi: 10.48550/arXiv.astro-ph/9601005

de Vaucouleurs, G. 1959, Handbuch der Physik, 53, 275, doi: 10.1007/978-3-642-45932-0_7

de Vaucouleurs, G., de Vaucouleurs, A., Corwin, Jr., H. G., et al. 1991, Third Reference Catalogue of Bright Galaxies

Graham, A. W., Driver, S. P., Petrosian, V., et al. 2005, AJ, 130, 1535, doi: 10.1086/444475

Graham, A. W., Erwin, P., Caon, N., & Trujillo, I. 2001a, ApJ, 563, L11, doi: 10.1086/338500

Graham, A. W., Trujillo, I., & Caon, N. 2001b, AJ, 122, 1707, doi: 10.1086/323090

Hernández-Toledo, H. M., Avila-Reese, V., Conselice, C. J., & Puerari, I. 2005, AJ, 129, 682, doi: 10.1086/427134

Hidalgo-Gámez, A. M. 2004, RMxAA, 40, 37

Hodge, P. W., & Kennicutt, Jr., R. C. 1983, ApJ, 267, 563, doi: 10.1086/160893

Hubble, E. P. 1926, ApJ, 64, 321, doi: 10.1086/143018

—. 1936, Realm of the Nebulae (New Haven: Yale Univ. Press)

Karachentsev, I. D., Karachentseva, V. E., & Huchtmeier, W. K. 2006, A&A, 451, 817, doi: 10.1051/0004-6361:20054497

Karachentsev, I. D., Makarov, D. I., Sharina, M. E., et al. 2003, A&A, 398, 479, doi: 10.1051/0004-6361:20021598

Magaña-Serrano, M. A., Hidalgo-Gámez, A. M., Vega-Acevedo, I., & Castañeda, H. O. 2020, RMxAA, 56, 39, doi: 10.22201/ia.01851101p.2020.56.01.06

Morgan, W. W. 1958, PASP, 70, 364, doi: 10.1086/127243

—. 1959, PASP, 71, 394, doi: 10.1086/127415

Nilson, P. 1973, Nova Acta Regiae Soc. Sci. Upsaliensis Ser. V, 0

Parkash, V., Brown, M. J. I., Jarrett, T. H., & Bonne, N. J. 2018, ApJ, 864, 40, doi: 10.3847/1538-4357/aad3b9

Pović, M., Sánchez-Portal, M., Pérez García, A. M., et al. 2009, ApJ, 702, L51, doi: 10.1088/0004-637X/702/1/L51

Roye, E. W., & Hunter, D. A. 2000, AJ, 119, 1145, doi: 10.1086/301265

Schade, D., Lilly, S. J., Crampton, D., et al. 1995, ApJ, 451, L1, doi: 10.1086/309677

Schuster, W. J., & Parrao, L. 2001, RMxAA, 37, 187

Sérsic, J. L., Pastoriza, M., & Carranza, G. 1968, BAAAR, 13, 20

van den Bergh, S., Abraham, R. G., Ellis, R. S., et al. 1996, AJ, 112, 359, doi: 10.1086/118020

Vega-Acevedo, I. 2013, Ms thesis, Estudio del parámetro de asimetría en galaxias espirales enanas, Instituto Politécnico Nacional, Ciudad de México, México

Vega-Acevedo, I., & Hidalgo-Gámez, A. M. 2022, RMxAA, 58, 61, doi: 10.22201/ia.01851101p.2022.58.01.05

Warmels, R. H. 1992, in ASPC, Vol. 25, Astronomical Data Analysis Software and Systems I, ed. D. M. Worrall, C. Biemesderfer, & J. Barnes, 115